

Article

Solubility of Gallic Acid in Single and Mixed Solvents

Yea-Rok Park and Bong-Seop Lee * 

Department of Chemical Engineering, Kangwon National University, Chuncheon 24341, Republic of Korea

* Correspondence: bslee0425@kangwon.ac.kr; Tel.: +82-33-250-6332

Abstract: Gallic acid, known for its biological activity contributing to human health, including antioxidant, anti-inflammatory, anticancer, and antimutagenic properties, was the focus of this study. The solubility of gallic acid was experimentally measured in pure and mixed solvents of water, ethanol, and acetic acid and predicted using the COSMO-SAC model and the Hansen solubility parameter. The Hansen solubility parameter method predicted a higher solubility of gallic acid in pure water than in pure ethanol, and in a mixed solvent, it predicted the maximum solubility at 80% water content, showing different results from the experimental data trends. However, using the molar volume obtained from COSMO calculations resulted in a tendency that matched the experimental results. The results revealed higher solubility in ethanol compared to water, with the solubility in mixed solvent falling within the range between them. Using the same method, the Hansen solubility parameter obtained was applied to acetic acid/water and acetic acid/ethanol mixtures, and similar trends were observed compared to experimental data. In particular, gallic acid in the acetic acid/water mixture solvent exhibited maximum solubility, and this phenomenon was well-predicted. As the temperature increased, solubility in both pure and mixed solvents also increased. While the COSMO-SAC model effectively captured this trend, the predicted solubility values were slightly lower than the experimental data. The solubility trends depending on solvent types were confirmed by comparing the σ -profiles of each compound. The σ -profile of gallic acid closely resembled that of ethanol, and this result led to higher solubility than water and acetic acid. The maximum solubility in ethanol/water and acetic acid/water mixed solvents could be anticipated when two solvents with significant differences in their σ -profiles are mixed in an appropriate ratio.

Keywords: gallic acid; solubility; mixed solvent; Hansen solubility parameter; COSMO-SAC



Citation: Park, Y.-R.; Lee, B.-S.

Solubility of Gallic Acid in Single and Mixed Solvents. *Separations* **2024**, *11*, 36. <https://doi.org/10.3390/separations11010036>

Academic Editors: Patroklos Varelzizis, Olga Gortzi and Sotiris I. Patsios

Received: 1 January 2024

Revised: 16 January 2024

Accepted: 19 January 2024

Published: 22 January 2024



Copyright: © 2024 by the authors. Licensee MDPI, Basel, Switzerland. This article is an open access article distributed under the terms and conditions of the Creative Commons Attribution (CC BY) license (<https://creativecommons.org/licenses/by/4.0/>).

1. Introduction

In modern society, with the widespread awareness that the consumption of chemically synthesized foods, additives, and drugs is linked to chronic illnesses, natural foods, additives, and herbal medicines have started to gain significant recognition within the pharmaceutical, food, and cosmetics industries [1]. Accordingly, there is growing interest in bioactive compounds for the creation of authentic natural products [2]. Bioactive compounds possess a number of nutritionally beneficial effects, such as antioxidants, anticancer, anti-inflammatory, antiobesity, and antiviral [2–6]. Therefore, the development and advancement of bioactive compounds with nutritional value, such as carotenoids (lutein, zeaxanthin) and flavonoids, are still being continuously carried out. These bioactive compounds are mostly extracted from raw materials, such as plants, and then processed to become final products [3]. In order to accelerate the development and advancement of these bioactive compounds, it is important to choose a method to increase the efficiency of extracting compounds from the raw source, which is the plant [4]. Therefore, the research on it is ongoing [5,6].

In the case of bio-active compounds, they can be denatured at high temperatures and are easily susceptible to damage depending on the conditions, and the efficiency and efficacy vary depending on the extraction method, so it is also very important to select

the right extraction process. Representative examples include organic solvent extraction, supercritical fluid extraction (SFE) [7,8], and ultrasonic-assisted extraction (UAE) [9–11]. In the case of organic solvent extraction, the cost is low, and the yield is high depending on the type of organic solvent, but it may leave residues in the final product, which requires a lot of energy and cost for purification and may generate environmentally unfriendly wastewater [4]. For these reasons, research on extraction using supercritical fluid carbon dioxide (SCF-CO₂), which is environmentally friendly and can utilize carbon dioxide, is being conducted, but due to the characteristics of supercritical fluids, it involves processes conducted under high pressure, raising safety concerns and facing issues related to the very low solubility of certain compounds. In the case of ultrasonic-assisted extraction, the efficiency is increased by destroying the cell walls in plant cells with ultrasound to extract bio-active compounds existing in plant cells [10,11], but this also uses organic solvents, so it has similar problems to organic solvent extraction. Due to this situation, it is currently best to proceed by improving the existing extraction methods.

Among the many biologically active compounds, gallic acid is a substance that can be obtained by hydrolyzing tannin, which gives an astringent taste in wine and persimmon [12,13]. Gallic acid has been used in the production of blue ink and photographic developers, but it has recently emerged as a high-value compound with important biological activities such as antioxidant [14–19], anti-inflammatory [17–19], anticancer [20–23], and antimutagenicity [24]. In order to use these high-value biologically active compounds, extraction must be carried out in the most efficient and environmentally friendly way. For this purpose, the solubility data of solutes in the chosen extraction solvent are essential [25]. However, the solubility measurement at a certain temperature and pressure entails significant time and cost consumption.

In the extraction process, conducting simulations using thermodynamic predictive models alongside experiments becomes significantly meaningful and important when considering the cost, time, and manpower involved in experiments to optimize the solubility in the process variables such as composition, temperature, and pressure. Due to these reasons, various researchers are concurrently performing simulations along with extraction experiments in their studies. Tung et al. [26] compared the measured solubilities of certain active pharmaceutical ingredients (APIs) such as lovastatin, simvastatin, rofecoxib, and etoricoxib at room temperature (~22 °C) and 45 °C with the solubilities predicted by NRTL-SAC [27] and COSMO-SAC [28] models. Chen et al. [29] used the COSMO-SAC model to screen over 40 solvents (alkanes, arenes, ethers, esters, ketones, etc.) for the solvent extraction of Phenol to determine the optimal extraction solvent. Oliveira et al. [30] predicted the solubilities of hydrophobic biomolecules—quercetin, curcumin, and gallic acid—after adding deep eutectic solvents (DESs) as additives, using COSMO-SAC [28] and COSMO-RS [31] based on the measured solubilities. Mitesh et al. [32] utilized the COSMO-SAC model to calculate the equilibrium solubilities between ionic liquids and hydrocarbons when selecting ionic liquids as co-solvents for extracting aromatic hydrocarbons from aliphatic hydrocarbons. Silveira et al. [33] predicted additional solubilities using the COSMO-SAC model based on the solubilities extracted using methanol + ethanol and methanol + 2-propanol solvent mixtures for nicotinamide.

In this study, we try to emphasize the fusion of experimental data and simulation through the application of thermodynamic models to enhance process optimization and forecast solubilities across diverse extraction scenarios. As mentioned above, in order to use gallic acid as a pharmaceutical substance, it is necessary to consider the toxicity of the extraction solvent. In the case of common organic solvents, the residual extraction solvent cannot be ignored due to their toxicity. For experimental solubility determination, the solubility of gallic acid in solvents was measured in safe solvents for consumption, such as water, ethanol, acetic acid, and their mixtures. To investigate the temperature effect on the solubility in pure water, ethanol, and acetic acid, the solubilities were measured at 298.15 K, 308.15 K, 318.15 K, 328.15 K, and 338.15 K under atmospheric pressure. Additionally, the solubility of gallic acid in solvents with various water/ethanol, water/acetic acid, and

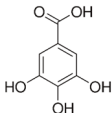
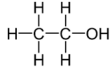
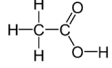
acetic acid/ethanol ratios were measured at 298.15 K, 318.15 K, and 338.15 K, respectively. The measured solubility data were compared with the predicted results using the Hansen solubility parameter method [34], which is a simple and long-standing approach with a theoretical framework, and COSMO-SAC [28], which is widely used to judge the affinity between the solute and the solvent [28,35–37].

2. Materials and Experiment

2.1. Materials

Gallic acid (99% purity, Shanghai, China) was purchased from ALADDIN and was used without additional purification. Ethyl alcohol (99.9% purity) and acetic acid (99.7% purity) were obtained from DAEJUNG, and deionized water (DI water) was prepared by Direct-Q® Water Purification System (Millipore Corporation, Burlington, MA, USA). The purity and supplier for used chemicals are reported in Table 1.

Table 1. Information on chemical materials and their suppliers.

Chemical Material	CAS Number	Structure	Molecular Weight [g/mol]	Source	Purity [%]
Gallic acid (C ₇ H ₆ O ₅)	149-91-7		170.12	ALADDIN, China	99
Ethyl alcohol (C ₂ H ₆ O)	64-17-5		46.069	DAEJUNG, Republic of Korea	Anhydrous, 99.9
Acetic acid (C ₂ H ₄ O ₂)	64-19-7		60.052	DAEJUNG, Republic of Korea	99.7

2.2. Solubility Measurement

The solubility of gallic acid was determined by measuring maximum absorbance using a UV–Vis spectrophotometer (Shimadzu UV-2600i, Kyoto, Japan) with quartz cells in the absorption wavelength range of 200–400 nm. For quantitative analysis of Gallic acid, a calibration curve ($R^2 = 0.9997$) was determined over a concentration range of standard solution at 5–80 ppm (w/w). The standard solution was produced by continuous dilution of stock solution (1000 ppm (w/w)). Absorbance measurement was carried out at 267 nm for gallic acid. To determine the solubility, the shake-flask method is used. A schematic diagram for measuring solubility is shown in Figure 1.

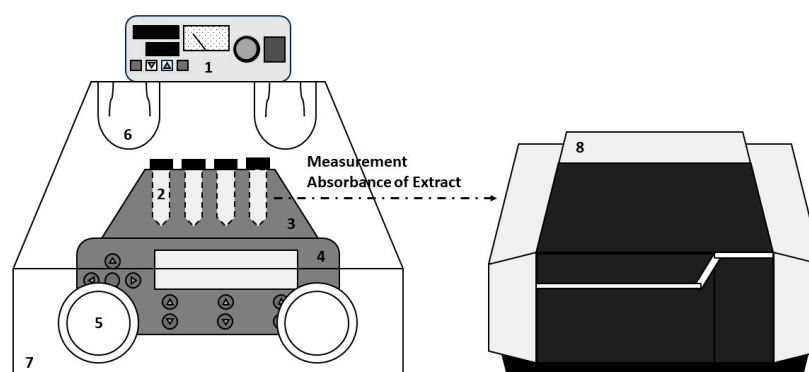


Figure 1. The apparatus for solubility measurement: (1) temperature controller for air bath, (2) conical glass centrifuge tube, (3) thermoblock, (4) thermomixer, (5) rubber glove, (6) quartz lamp, (7) air bath, and (8) UV–Vis spectrophotometer.

To prepare the solution, three different solvents were used: DI water, pure ethanol, and a solvent mixture of deionized water and ethanol. The solvents were mixed in various

molar ratios, and the weight of all solvents was carefully measured using an analytical balance (METTLER TOLEDO, Greifensee, Swiss, ME204). The mixed solvent was injected into a conical glass centrifuge tube, and excess solute was added to the solvent to create a supersaturated solution. The centrifuge tube was then placed in a ThermoMixer C (Eppendorf, Hamburg, Germany, 15 mL heating block) set to a constant temperature. The amount of excess solute was also accurately weighed using an analytical balance. The saturated solution was stirred in a heating block at a specified stirring speed for 16 h (600 rpm). After stirring, it was left undisturbed for 6 h to allow the saturated solution to settle. The supernatant was extracted using a glass syringe fitted with a syringe filter (PTFE, pore 0.45 μm), and the solubility was measured from the calibration curve of the absorbance using a UV-Vis spectrophotometer. The absorbance wavelength range measured for solubility measurement was 200–400 nm. To prevent precipitation of chlorogenic acid caused by temperature changes during extraction, the orbital shaking heating block was located in a glove box with temperature control. The air temperature inside the glove box was maintained at 5 $^{\circ}\text{C}$ higher than the extraction temperature, and the air was circulated using a fan to maintain a uniform temperature. Water was chosen as the dilute solvent because, unlike ethanol, it does not volatilize and is a solvent that is cut off in the UV-Vis spectrophotometer used in this experiment. A diluted solution was prepared in 0.1 mL of the extraction solution using a different dilution ratio (approximately 2500–7000 times) for each temperature.

2.3. Thermal Analysis

TGA (TA Instruments, New Castle, DE, USA, TGA 55) was used to investigate thermal stability and to determine the temperature range for differential scanning calorimetry measurement. TGA was measured in a temperature range of room temperature to 800 $^{\circ}\text{C}$ using nitrogen as a purging gas at a heating rate of 20 $^{\circ}\text{C}/\text{min}$. To determine the melting enthalpy and melting point values, DSC (TA Instruments, DSC25 + RCS: refrigerated cooling system 90) was used.

3. Theory and Model

3.1. COSMO-SAC Model

The solubility of gallic acid (i) in solution is estimated from the equality of fugacity of the gallic acid in the solid and the solution phases under constant temperature T and pressure P . From the thermodynamic relationship, the solubility of a gallic acid in solution can be calculated from [38]

$$\ln x_i = -\ln \gamma_i + \frac{\Delta H_f}{RT_m} \left(1 - \frac{T_m}{T} \right) \quad (1)$$

where the T_m and ΔH_f of the gallic acid are obtained by measurement with DSC. Then, the activity coefficient of the gallic acid in the liquid phase is determined by the COSMO-SAC model [39].

The COSMO-SAC model [39] describes the activity coefficient due to interactions between molecules in contact, including a combinatorial ($comb$) and a residual (res) term,

$$\ln \gamma_i^{COSMO-SAC} = \ln \gamma_i^{res} + \ln \gamma_i^{comb} \quad (2)$$

The residual term describes non-ideal interactions due to differences in the attractive molecular interactions. In the COSMO-SAC model, this term is determined by the screening charge on the molecular surface. The arrangement of these screening charges on the molecular surface is derived from the COSMO calculations [28]. In these calculations, the molecule is dissolved in an ideal conductor. The electronic characteristics of the molecule manifest through induced screening charges on the surface of the cavity. To quantify the distribution of the screening charges, the molecular surface is divided into small segments. Additionally, the molecule's surface is categorized into three types: non-

hydrogen-bonding (nHB) surfaces, hydrogen-bonding (OH) surfaces from -OH groups in alcohols and water, and any other hydrogen-bonding (OT) surfaces, such as carboxylic acid (-COOH), carbonyl groups (C=O), and amide groups (-NH₂) [39]. The combinatorial term describes the non-ideality of molecules based on differences in size and shape using the Staverman–Guggenheim relationship [40].

3.2. Hansen Solubility Parameter

Hildebrand and Scott [41] experimentally confirmed the hypothesis that solvents dissolve solutes that are similar to themselves more effectively. They introduced the Hildebrand solubility parameter, δ , as an experimental solubility parameter; however, Hildebrand’s parameter only represented the cohesion energy between the solute and the solvent. Hansen [42] modified this into the Hildebrand–Hansen solubility parameter. Hansen categorized the energy used by Hildebrand, the cohesion energy, into three types: first, δ_d for dispersion forces; second, δ_p for polarity; and finally, δ_h for hydrogen bonds between molecules.

$$\delta_d = \frac{\sum_i F_{d,i}}{\sum_i V_i}; \delta_p = \frac{(\sum_i F_{p,i}^2)^{1/2}}{\sum_i V_i}; \delta_h = \left(\frac{\sum_i E_{h,i}}{\sum_i V_i} \right)^{1/2} \tag{3}$$

The $F_{d,i}$, $F_{p,i}$, $E_{h,i}$, and V_i values are obtained from the group contribution method [34] and COSMO calculation. The Hansen solubility parameters obtained through two different methods are presented in Table 2. The sum of these three types of solubility parameters represents the total solubility parameter, expressed by the following equation:

$$\delta^2 = \delta_d^2 + \delta_p^2 + \delta_h^2 \tag{4}$$

The difference between the Hansen solubility parameters of the solute and the solvent can be represented by the Euclidean distance, as shown below [42]

$$\Delta\delta_{ij} = \sqrt{4(\delta_d^i - \delta_d^j)^2 + (\delta_p^i - \delta_p^j)^2 + (\delta_h^i - \delta_h^j)^2} \tag{5}$$

where superscript i represents the solute, and j denotes the solvent (either pure solvent or mixed solvent). The three Hansen solubility parameters can be estimated through the group contribution method known as the Hoftyzer–Van Krevelen method [34]. The solubility parameter when using a solvent mixture composed of water and ethanol as the mixed solvent (j) is calculated using the equation below [43].

$$\delta_j = \phi\delta_m + (1 - \phi)\delta_n \tag{6}$$

where subscripts m and n represent solvent 1 and solvent 2, respectively. ϕ indicates the volume fraction of m in the mixed solvents (j) of m and n .

Table 2. Calculation results of Hansen solubility parameter.

Chemicals		δ_d [MPa] ^{1/2}	δ_p [MPa] ^{1/2}	δ_h [MPa] ^{1/2}	δ_t [MPa] ^{1/2}	References
Group contribution	Gallic acid	33.0	17.2	35.4	51.4	This study
	Water	15.6	16.0	42.3	47.8	[42]
	Ethanol	15.8	8.8	19.4	26.5	[42]
	Acetic acid	14.5	8.0	13.5	21.4	[42]
COSMO	Gallic acid	17.19	8.99	25.57	32.10	This study
	Water	15.6	16.0	42.3	47.8	This study
	Ethanol	21.31	11.84	21.76	32.67	This study
	Acetic acid	20.46	20.42	22.12	36.40	This study

4. Results

Prior to measuring the solubility of gallic acid in solvents, a calibration curve was prepared for gallic acid calibration. Considering the detection limit of the UV-Vis spectrophotometer, the standard solutions up to 80 ppm [mg/kg] were prepared, and their absorbance was measured. The measured absorbance for standard solutions is shown in Figure 2, and the maximum absorption of gallic acid was observed at 267 nm. Figure 3 depicts the calibration curve. The determination coefficient is the value of 0.9997, meaning that linearity is high.

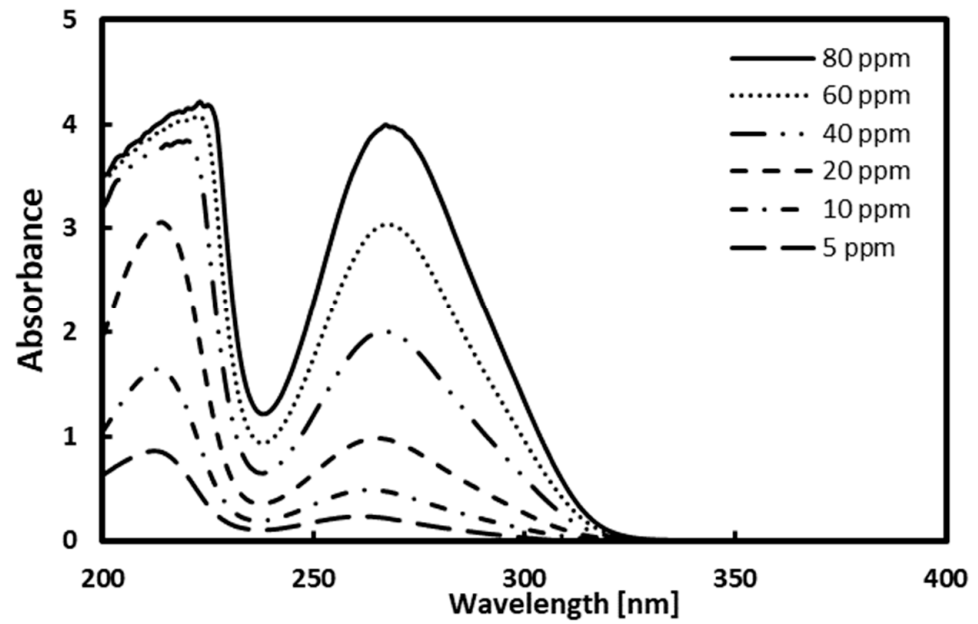


Figure 2. Absorbance results of gallic acid at 267 nm.

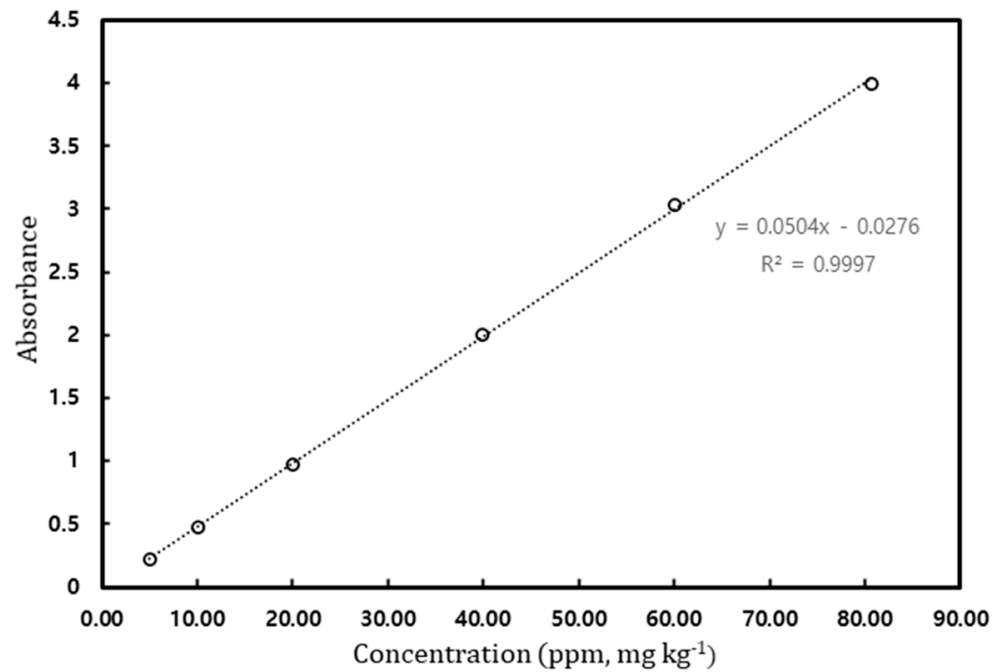


Figure 3. Calibration curve of gallic acid.

4.1. Thermal Analysis

Prior to measuring using differential scanning calorimetry (DSC), thermogravimetric analyzer (TGA) analysis was conducted by ramping from 293.15 K to 1273.15 K at a rate of 20.00 K/min to confirm the decomposition temperature of gallic acid. A significant weight loss was observed around 373.15 K, attributed to the loss of moisture in the sample. Therefore, gallic acid was dried at 313.15 K for 24 h using a vacuum oven (JEIO TECH, Deajeon, Republic of Korea, VO-10X) before proceeding with DSC measurements. DSC measurements were calibrated by using the difference between the measured value ($T_m = 156.981\text{ }^\circ\text{C}$) and the reference melting temperature ($T_m = 156.60\text{ }^\circ\text{C}$) of indium as the reference material. The melting point and melting enthalpy of gallic acid measured by DSC were reported in Table 3 with values from the literature [44–46] and were carried out from 303.25 K to 673.15 K at a ramp rate of 10.0 K/min. The standard uncertainty u for melting temperature is $u(T) = 0.4\text{ K}$ and is estimated by the guidelines of NIST [47]. Furthermore, the group contribution method [48] was employed to estimate the melting enthalpy and melting temperature, demonstrating values closely aligned with experimental results. The TGA and DSC measurement results are presented in Figure 4.

Table 3. Melting temperatures and melting enthalpies of gallic acid measured by DSC.

Melting Temperature [K]	Melting Enthalpy [kJ/mol]	References
533.64	102.59	This work
545.85	64.54	Xue et al. [44]
539.62	94.36	Celep et al. [45]
535.84	60.68	Singh et al. [46]
538.66	97.64	Group contribution method [48]

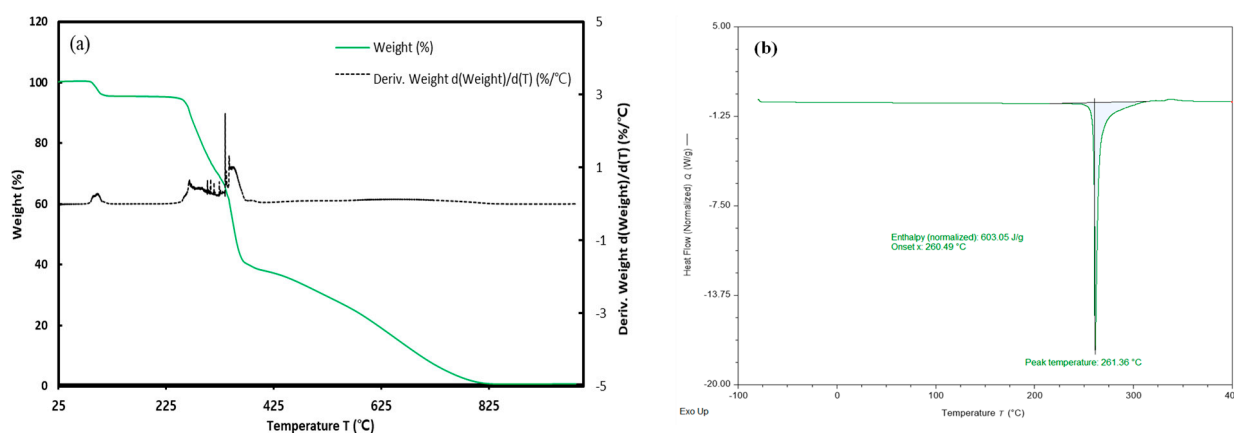


Figure 4. Thermal analysis (a) TGA and (b) DSC measurement of gallic acid.

4.2. Solubility in Pure and Mixed Solvents

In the case of pure solvents, solubility measurements were carried out at five temperature points of 298.15 K, 308.15 K, 318.15 K, 328.15 K, and 338.15 K under atmospheric pressure conditions and were performed at least twice. The measured solubility data are reported in Table 4. Figure 5 depicts the solubility of gallic acid in pure solvent at different temperatures. As shown in Figure 5, the solubility of gallic acid in pure water and ethanol, measured in this work, exhibited a relatively good agreement with solubility data measured by many researchers [49–54].

The solubility of gallic acid in ethanol exhibited a phenomenon of gradually increasing with temperature, and this phenomenon is greater than changes in solubility in water. Although the COSMO-SAC model accurately depicted the trend of solubility with temperature, it significantly underpredicted the values compared to experimental data. The solubility in the mixed solution was measured at 298.15 K, 318.15 K, and 338.15 K

under atmospheric pressure conditions, and the results are presented in Tables 5–7 for water/ethanol, water/acetic acid, and acetic acid/ethanol mixed solvents, respectively. As shown in Figure 6a, it can be observed that the solubility of gallic acid decreases as the water content in water/ethanol mixed solvent increases. The results obtained in this study showed a tendency consistent with the literature data reported by Noubigh et al. [55], but the solubility data reported in this study were slightly higher at the low ethanol concentration range. Additionally, at higher temperatures, it is evident that the decrease in solubility of gallic acid due to increased water content is more pronounced. The significant decrease in the solubility of gallic acid in the presence of water in the mixed solvent, especially when the water fraction is above 0.4, suggests that water acts as an antisolvent for gallic acid in ethanol, leading to a salting-out effect. In other words, ethanol acts as a co-solvent for the solubility of gallic acid in water. As shown in Figure 6b, the solubility of gallic acid in acetic acid/water mixed solvent initially increased with an increase in the concentration of acetic acid, reaching its maximum solubility before decreasing. The predictions of the COSMO-SAC model also indicated the maximum solubility, although the predicted maximum composition point was somewhat higher. Figure 6c depicts the solubility of gallic acid in acetic acid/ethanol mixed solvent, where the solubility gradually decreased with an increase in the concentration of acetic acid. This trend was well-captured by the COSMO-SAC model as well.

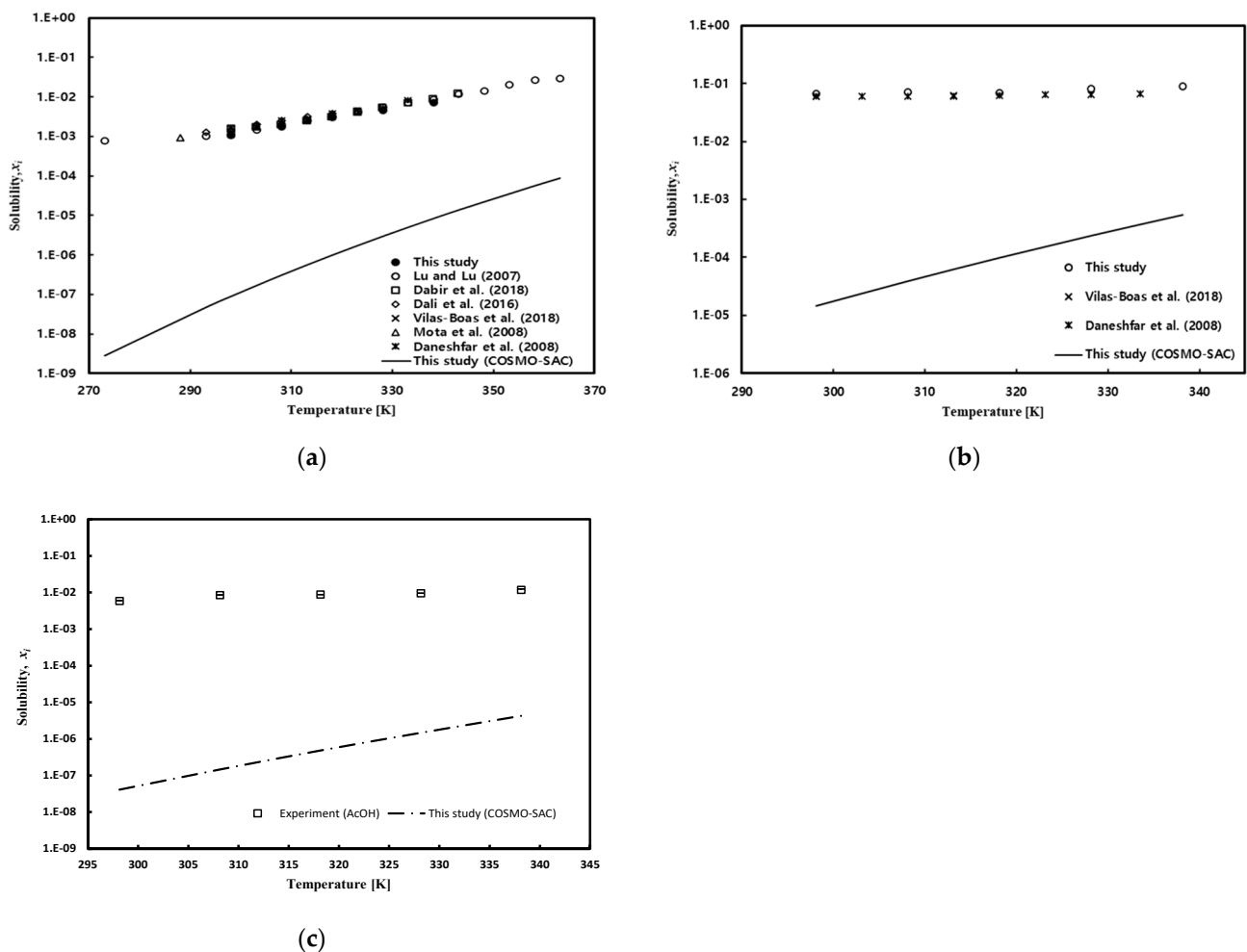


Figure 5. Temperature effect on gallic acid solubility in (a) pure water: Lu and Lu [49] (open circle), Dabir et al. [53] (open square), Dali et al. [52] (open diamond), Vilas-Boas et al. [54] (cross), Mota et al. [51] (open triangle), and Daneshfar et al. [50] (star); (b) ethanol: Vilas-Boas et al. [54] (cross) and Daneshfar et al. [50] (star); and (c) acetic acid.

Table 4. The gallic acid solubilities in pure solvents (i.e., ethanol, water, and acetic acid).

Temp. * [K]	Solubility in Ethanol		Solubility in Water		Solubility in Acetic Acid	
	ppm [mg/kg]	Mole Fraction	ppm [mg/kg]	Mole Fraction	ppm [mg/kg]	Mole Fraction
298.15	$207,146.50 \pm 1.35 \times 10^4$	$0.0661 \pm 5.09 \times 10^{-3}$	$10,519.97 \pm 5.47 \times 10^2$	$0.0011 \pm 5.90 \times 10^{-5}$	$16,497.12 \pm 3.36 \times 10^2$	$0.0059 \pm 1.21 \times 10^{-4}$
308.15	$219,026.47 \pm 4.04 \times 10^3$	$0.0706 \pm 1.55 \times 10^{-3}$	$16,539.57 \pm 3.88 \times 10^3$	$0.0018 \pm 4.24 \times 10^{-4}$	$23,576.01 \pm 5.36 \times 10^2$	$0.0085 \pm 1.95 \times 10^{-4}$
318.15	$216,239.13 \pm 1.06 \times 10^4$	$0.0695 \pm 4.05 \times 10^{-3}$	$28,517.65 \pm 4.00 \times 10^3$	$0.0031 \pm 4.44 \times 10^{-4}$	$24,433.05 \pm 8.67 \times 10^1$	$0.0088 \pm 3.16 \times 10^{-5}$
328.15	$244,750.77 \pm 2.10 \times 10^4$	$0.0807 \pm 8.41 \times 10^{-3}$	$40,776.08 \pm 9.50 \times 10^3$	$0.0045 \pm 1.08 \times 10^{-3}$	$26,432.66 \pm 3.44 \times 10^2$	$0.0095 \pm 1.26 \times 10^{-4}$
338.15	$266,708.60 \pm 1.07 \times 10^4$	$0.0897 \pm 4.43 \times 10^{-3}$	$63,324.04 \pm 2.43 \times 10^4$	$0.0071 \pm 2.86 \times 10^{-3}$	$32,698.30 \pm 1.94 \times 10^3$	$0.0118 \pm 7.14 \times 10^{-4}$

* The standard uncertainty u for temperature is $u(T) = 0.5$ K and is estimated by the guidelines of NIST [47].

Table 5. The solubilities of gallic acid in different mixed solvents (water + ethanol).

Temp.* [K]	Weight Fraction of Water	Solubility in Mixed Solvents	
		ppm [mg/kg]	Mole Fraction
298.15	0.1992	$171,062.66 \pm 1.28 \times 10^3$	0.0391 ± 0.0003
	0.3973	$132,922.31 \pm 1.21 \times 10^3$	0.0237 ± 0.0002
	0.6074	$76,377.44 \pm 7.01 \times 10^1$	0.0109 ± 0.0001
	0.8087	$27,100.20 \pm 2.60 \times 10^2$	0.0033 ± 0.0001
318.15	0.1910	$213,151.74 \pm 6.68 \times 10^3$	0.0506 ± 0.0019
	0.3762	$179,696.23 \pm 1.29 \times 10^3$	0.0335 ± 0.0003
	0.5985	$125,294.71 \pm 4.59 \times 10^3$	0.0184 ± 0.0008
	0.7763	$65,494.35 \pm 1.05 \times 10^3$	0.0082 ± 0.0001
338.15	0.1740	$275,996.62 \pm 5.69 \times 10^2$	0.0699 ± 0.0001
	0.3403	$257,167.66 \pm 9.42 \times 10^3$	0.0518 ± 0.0024
	0.5198	$209,719.19 \pm 6.52 \times 10^3$	0.0343 ± 0.0013
	0.7115	$144,023.67 \pm 8.39 \times 10^3$	0.0195 ± 0.0013

* The standard uncertainty u for temperature is $u(T) = 0.5$ K and is estimated by the guidelines of NIST [47].

Table 6. The solubilities of gallic acid in different mixed solvents (water + acetic acid).

Temp.* [K]	Weight Fraction of Water	Solubility in Mixed Solvents	
		ppm [mg/kg]	Mole Fraction
298.15	0.1848	$30,326.71 \pm 6.99 \times 10^2$	$0.0076 \pm 1.79 \times 10^{-4}$
	0.3720	$38,269.95 \pm 1.25 \times 10^2$	$0.0073 \pm 2.47 \times 10^{-5}$
	0.5597	$40,188.55 \pm 2.69 \times 10^2$	$0.0062 \pm 4.31 \times 10^{-5}$
	0.7661	$28,551.78 \pm 2.68 \times 10^2$	$0.0036 \pm 3.50 \times 10^{-5}$
318.15	0.1803	$53,892.58 \pm 3.00 \times 10^2$	$0.0137 \pm 7.97 \times 10^{-5}$
	0.3598	$69,692.63 \pm 1.10 \times 10^3$	$0.0137 \pm 2.30 \times 10^{-4}$
	0.5393	$75,314.83 \pm 6.29 \times 10^2$	$0.0120 \pm 1.07 \times 10^{-4}$
	0.7989	$63,058.33 \pm 7.13 \times 10^0$	$0.0083 \pm 9.93 \times 10^{-7}$
338.15	0.1732	$91,435.66 \pm 8.14 \times 10^2$	$0.0240 \pm 2.29 \times 10^{-4}$
	0.3365	$129,925.60 \pm 1.15 \times 10^4$	$0.0270 \pm 2.68 \times 10^{-3}$
	0.5037	$136,361.92 \pm 1.14 \times 10^3$	$0.0231 \pm 2.18 \times 10^{-4}$
	0.6967	$116,533.44 \pm 1.98 \times 10^4$	$0.0161 \pm 3.05 \times 10^{-3}$

* The standard uncertainty u for temperature is $u(T) = 0.5$ K and is estimated by the guidelines of NIST [47].

Table 7. The solubilities of gallic acid in different mixed solvents (ethanol + acetic acid).

Temp.* [K]	Weight Fraction of Ethanol	Solubility in Mixed Solvents	
		ppm [mg/kg]	Mole Fraction
298.15	0.1511	$37,562.70 \pm 1.46 \times 10^3$	$0.0130 \pm 5.18 \times 10^{-4}$
	0.3183	$47,164.67 \pm 2.15 \times 10^3$	$0.0156 \pm 7.35 \times 10^{-4}$
	0.4871	$80,453.04 \pm 3.25 \times 10^2$	$0.0259 \pm 1.11 \times 10^{-4}$
	0.6464	$134,836.53 \pm 3.28 \times 10^3$	$0.0429 \pm 1.15 \times 10^{-3}$
318.15	0.1509	$38,694.22 \pm 2.56 \times 10^2$	$0.0134 \pm 9.09 \times 10^{-5}$
	0.3130	$62,953.53 \pm 5.89 \times 10^2$	$0.0211 \pm 2.06 \times 10^{-4}$
	0.4756	$102,236.67 \pm 1.51 \times 10^3$	$0.0335 \pm 5.32 \times 10^{-4}$
	0.6286	$158,699.01 \pm 8.63 \times 10^2$	$0.0515 \pm 3.16 \times 10^{-4}$
338.15	0.1479	$57,627.62 \pm 2.23 \times 10^3$	$0.0202 \pm 8.11 \times 10^{-4}$
	0.3032	$92,373.61 \pm 1.08 \times 10^3$	$0.0316 \pm 3.94 \times 10^{-4}$
	0.4550	$141,140.64 \pm 2.15 \times 10^3$	$0.0476 \pm 8.05 \times 10^{-4}$
	0.6090	$185,019.32 \pm 3.05 \times 10^4$	$0.0613 \pm 1.16 \times 10^{-2}$

* The standard uncertainty u for temperature is $u(T) = 0.5$ K and is estimated by the guidelines of NIST [47].

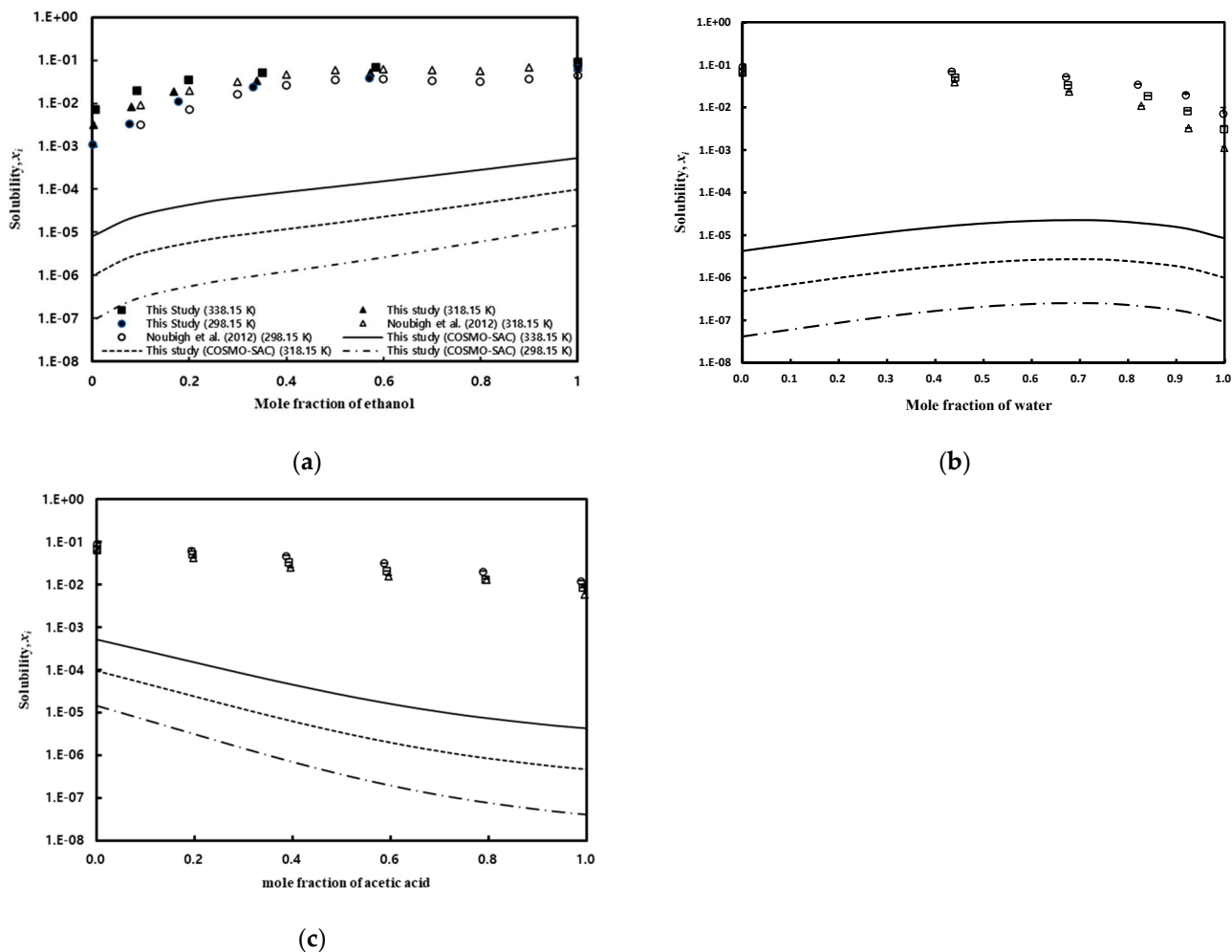


Figure 6. Effect of temperature and the ratio of mixed solvents on gallic acid solubility in mixed solvents: (a) water/ethanol, Noubigh et al. [55] (open circle and open triangle); (b) water/acetic acid; and (c) acetic acid/ethanol.

The Hansen solubility parameter of gallic acid was calculated through the Hoftzyer–Van Krevelen method [43], and the values of the Hansen solubility parameter for the solvents (water, ethanol) were obtained from reference [42]. The Hansen solubility parameter represents the miscibility between the solute and the solvent rather than the actual solubility. A smaller difference in the solubility parameters between the solute and the solvent indicates a more active interaction, suggesting higher miscibility between them. In other words, a higher miscibility between the solute and the solvent implies a higher solubility. Figure 7 depicts a comparison between the Hansen solubility parameter and the experimental data. Figure 7a shows the molar volume of each component estimated using the Hoftzyer–Van Krevelen method [43] for predicting Hansen solubility parameters. Figure 7b presents the results obtained through COSMO calculation [28,56]. Mahmoudabadi and Pazuki [57] have pointed out the discrepancies between the values obtained for the molar volumes of pharmaceutical compounds and solvents using the group contribution method in Barton [58] and COSMO calculations. As can be seen in Figure 7, as you can see, the method calculated by the Hoftzyer–Van Krevelen method predicted a high solubility of gallic acid in pure water. It also showed maximum solubility at 80% water content. Meanwhile, the method based on COSMO calculations tended to align accurately with experimental tendency. These results indicate that the molar volumes estimated using the Hoftzyer–Van Krevelen method are not accurate, particularly concerning components with benzene groups. This suggests caution when applying this method to such aromatic components, a trend that has also been noted by other researchers [59].

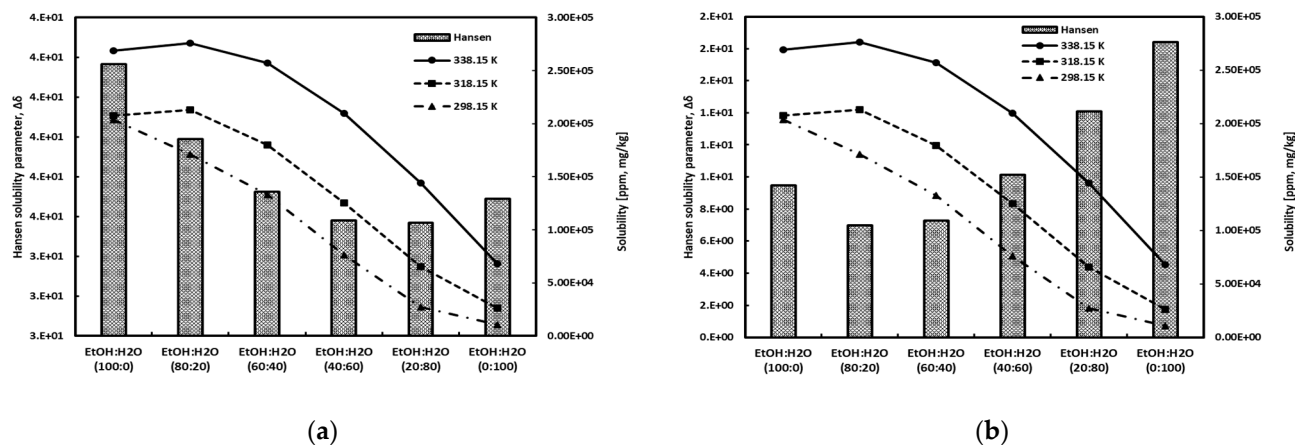


Figure 7. Comparison of the experimental data and the Hansen solubility parameter using molar volume obtained from (a) Hoftyzer–Van Krevelen method [34] and from (b) COSMO calculation.

Figure 8 compares the measured solubility of gallic acid in mixed solvents of acetic acid with water and ethanol to the results predicted by the Hansen solubility parameter method. In this case, the Hansen solubility parameter utilized the molar volume obtained through COSMO calculations. As shown in Figure 8a, in acetic acid/water mixed solvents, the solubility of gallic acid exhibited a trend of increasing to a maximum solubility point and then decreasing as the concentration of water increased. The experimental results and predictions from the Hansen solubility parameter method showed similar behavior. On the other hand, as illustrated in Figure 8b, in acetic acid/ethanol mixed solvents, the solubility of gallic acid showed a gradual increase with an increase in the ethanol content. This trend was well-predicted by the Hansen solubility parameter method.

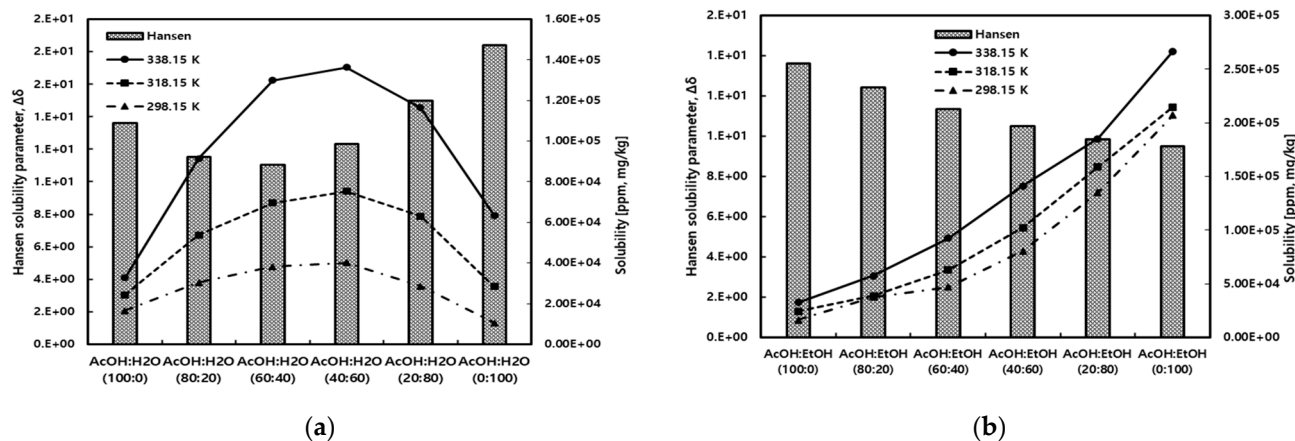


Figure 8. Comparison of gallic acid solubility for experimental and Hansen solubility parameter method in (a) acetic acid/water and (b) acetic acid/ethanol mixed solvents.

The solubility difference of gallic acid in pure solvents and the solubility trend in mixed solvents can be explained by comparing the σ -profile. As shown in Figure 9, the σ -profile for non-hydrogen bonding in gallic acid is about three times larger than that of hydrogen bonds. This suggests that van der Waals interactions, which are non-hydrogen bonding interactions, play an important role in interactions between gallic acid and solvents [37].

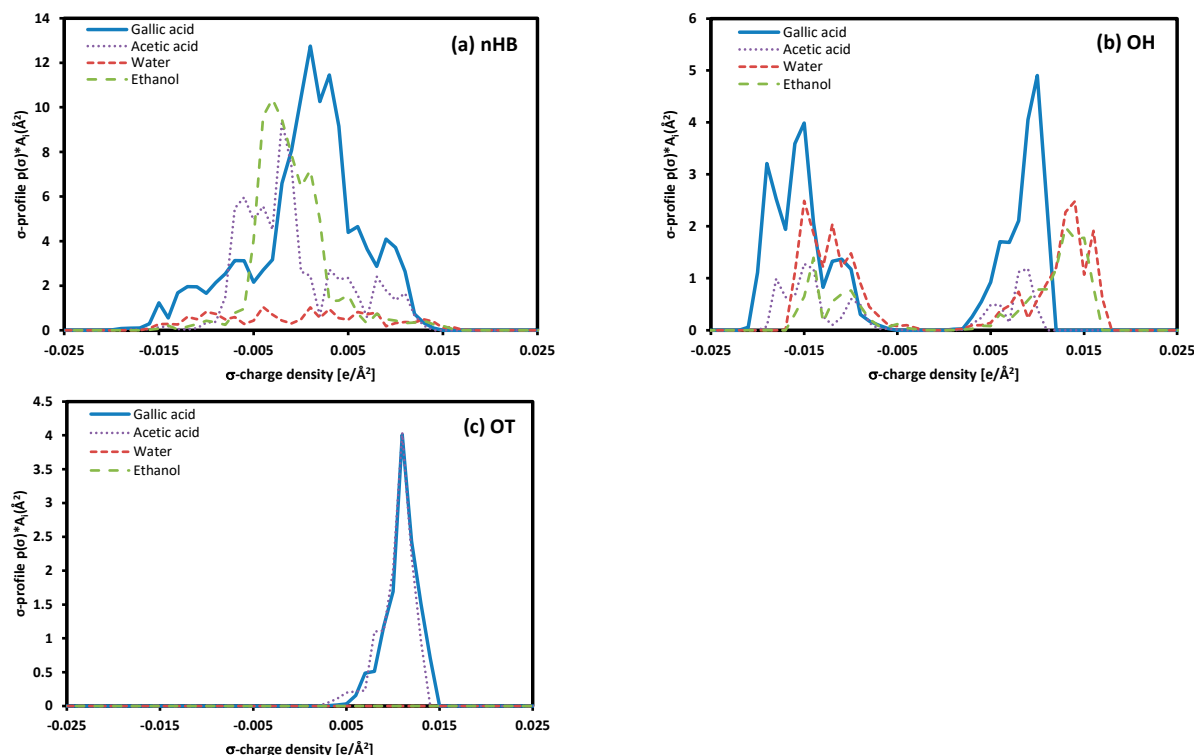


Figure 9. The σ -profile of each component.

The solubility difference between water and ethanol can be explained by comparing the σ -profile, which represents the surface charge density of molecules. Around the 0 σ -charge density area, the σ -profile of gallic acid shows a more similar trend to ethanol and acetic acid than water, with a significant difference. This difference can be confirmed by the higher solubility of gallic acid in ethanol. When considering the phenomenon of maximum solubility in ethanol/water and acetic acid/water mixed solvents based on the σ -profiles of each component, it can be anticipated that the maximum solubility occurs when two solvents with significant differences in their σ -profiles are mixed in an appropriate ratio. This phenomenon is also confirmed in the research results of Lee and Lin [37]. On the other hand, due to the relatively small difference in the σ -profiles for ethanol and acetic acid, the solubility of gallic acid is situated within the range between pure ethanol and acetic acid when dissolved in a mixed solvent.

5. Conclusions

This study measured the solubility of gallic acid, a biologically active compound contributing to human health improvement, and compared it with the predicted values using the COSMO-SAC model and the Hansen solubility parameter method. The solubility of gallic acid in pure solvents, water, and ethanol showed an increasing trend with temperature. The COSMO-SAC model predicted solubility values lower than the experimental values but well-captured the temperature-dependent trends. In mixed solvents, the solubility of gallic acid exhibited a sequential decrease as the water concentration increased, and this trend remained consistent at different temperatures (i.e., 298.15 K, 318.15 K, and 338.15 K). The Hansen solubility parameter method predicted a higher solubility of gallic acid in pure water than in pure ethanol, and in a mixed solvent, it predicted the maximum solubility at 80% water content, showing different results from the experimental data trend. However, using the molar volume obtained from COSMO calculations resulted in a tendency that matched the experimental results. These results indicate that the molar volume of gallic acid estimated by the Hoftyzer–Van Krevelen method is not appropriate. Using the molar volume obtained from COSMO calculations, the Hansen solubility parameter obtained was applied to acetic acid/water and acetic acid/ethanol mixtures, and similar trends were

observed compared to experimental data. In particular, gallic acid in the acetic acid/water mixture solvent exhibited maximum solubility, and this phenomenon was well-predicted. The COSMO-SAC model accurately described this trend but predicted solubility lower than the experimental data. The solubility trends in both pure and mixed solvents were confirmed through a comparison of the σ -profiles of each compound. The σ -profile of gallic acid closely resembled that of ethanol, and this result led to higher solubility than water and acetic acid. The maximum solubility in ethanol/water and acetic acid/water mixed solvents could be anticipated when two solvents with significant differences in their σ -profiles are mixed in an appropriate ratio.

Author Contributions: Y.-R.P.: data curation and original draft preparation; B.-S.L.: writing—review and editing, supervision, project administration, and funding acquisition. All authors have read and agreed to the published version of the manuscript.

Funding: This research was supported by the “Regional Innovation Strategy (RIS)” through the National Research Foundation of Korea (NRF), funded by the Ministry of Education (MOE) in 2023 (2022RIS-005). This study was supported by a 2021 research grant from the Kangwon National University. This work was also supported by the Korea Institute of Energy Technology Evaluation and Planning (KETEP) and the Ministry of Trade, Industry and Energy (MOTIE) of the Republic of Korea (No. 20224000000080).

Data Availability Statement: The data that support the findings of this study are available from the corresponding authors upon request.

Conflicts of Interest: The authors declare no conflicts of interest.

References

1. Mišić, D.; Zizovic, I.; Stamenić, M.; Ašanin, R.; Ristić, M.; Petrović, S.D.; Skala, D. Antimicrobial activity of celery fruit isolates and SFE process modeling. *Biochem. Eng. J.* **2008**, *42*, 148–152. [[CrossRef](#)]
2. Patil, B.S.; Jayaprakasha, G.K.; Chidambara Murthy, K.N.; Vikram, A. Bioactive compounds: Historical perspectives, opportunities, and challenges. *J. Agric. Food Chem.* **2009**, *57*, 8142–8160. [[CrossRef](#)]
3. Altemimi, A.; Lakhssassi, N.; Baharlouei, A.; Watson, D.G.; Lightfoot, D.A. Phytochemicals: Extraction, Isolation, and Identification of Bioactive Compounds from Plant Extracts. *Plants* **2017**, *6*, 42. [[CrossRef](#)] [[PubMed](#)]
4. Rasul, M.G. Conventional Extraction Methods Use in Medicinal Plants, their Advantages and Disadvantages. *Int. J. Basic. Sci. Appl. Comput.* **2018**, *2*, 10–14.
5. Smith, R.M. Before the injection—modern methods of sample preparation for separation techniques. *J. Chromatogr. A* **2003**, *1000*, 3–27. [[CrossRef](#)] [[PubMed](#)]
6. Azmir, J.; Zaidul, I.S.M.; Rahman, M.M.; Sharif, K.M.; Mohamed, A.; Sahena, F.; Jahurul, M.H.A.; Ghafoor, K.; Norulaini, N.A.N.; Omar, A.K.M. Techniques for extraction of bioactive compounds from plant materials: A review. *J. Food Eng.* **2013**, *117*, 426–436. [[CrossRef](#)]
7. da Silva, R.P.F.F.; Rocha-Santos, T.A.P.; Duarte, A.C. Supercritical fluid extraction of bioactive compounds. *TrAC Trends Anal. Chem.* **2016**, *76*, 40–51. [[CrossRef](#)]
8. Uwineza, P.A.; Waskiewicz, A. Recent Advances in Supercritical Fluid Extraction of Natural Bioactive Compounds from Natural Plant Materials. *Molecules* **2020**, *25*, 3847. [[CrossRef](#)]
9. Das, P.R.; Eun, J.B. A comparative study of ultra-sonication and agitation extraction techniques on bioactive metabolites of green tea extract. *Food Chem.* **2018**, *253*, 22–29. [[CrossRef](#)]
10. Rahman, M.M.; Lamsal, B.P. Ultrasound-assisted extraction and modification of plant-based proteins: Impact on physicochemical, functional, and nutritional properties. *Compr. Rev. Food Sci. Food Saf.* **2021**, *20*, 1457–1480. [[CrossRef](#)]
11. Liu, Y.; Liu, X.; Cui, Y.; Yuan, W. Ultrasound for microalgal cell disruption and product extraction: A review. *Ultrason. Sonochem.* **2022**, *87*, 106054. [[CrossRef](#)] [[PubMed](#)]
12. Mammela, P.; Tuomainen, A.; Savolainen, H.; Kangas, J.; Vartiainen, T.; Lindroos, L. Determination of gallic acid in wood dust as an indicator of oak content. *J. Environ. Monit.* **2001**, *3*, 509–511. [[CrossRef](#)]
13. Kim, T.J.; Silva, J.L.; Jung, Y.S. Enhanced functional properties of tannic acid after thermal hydrolysis. *Food Chem.* **2011**, *126*, 116–120. [[CrossRef](#)]
14. Yen, G.-C.; Duh, P.-D.; Tsai, H.-L. Antioxidant and pro-oxidant properties of ascorbic acid and gallic acid. *Food Chem.* **2002**, *79*, 307–313. [[CrossRef](#)]
15. KIM, Y.-J. Antimelanogenic and Antioxidant Properties of Gallic Acid. *Biol. Pharm. Bull.* **2007**, *30*, 1052–1055. [[CrossRef](#)] [[PubMed](#)]
16. Lu, Z.; Nie, G.; Belton, P.S.; Tang, H.; Zhao, B. Structure-activity relationship analysis of antioxidant ability and neuroprotective effect of gallic acid derivatives. *Neurochem. Int.* **2006**, *48*, 263–274. [[CrossRef](#)]

17. Kroes, B.H.; Berg, A.J.J.v.d.; Ufford, H.C.Q.v.; Dijk, H.v.; Labadie, R.P. Anti-Inflammatory Activity of Gallic Acid. *Planta Medica* **1992**, *58*, 499–504. [[CrossRef](#)] [[PubMed](#)]
18. Locatelli, C.; Filippin-Monteiro, F.B.; Centa, A.; Creczynsky-Pasa, T.B. *Antioxidant, Antitumoral and Anti-Inflammatory Activities of Gallic Acid*; Nova Publishers: Hauppauge, NY, USA, 2013; pp. 1–16.
19. Bai, J.; Zhang, Y.; Tang, C.; Hou, Y.; Ai, X.; Chen, X.; Zhang, Y.; Wang, X.; Meng, X. Gallic acid: Pharmacological activities and molecular mechanisms involved in inflammation-related diseases. *Biomed. Pharmacother.* **2021**, *133*, 110985. [[CrossRef](#)]
20. Maurya, D.K.; Nandakumar, N.; Devasagayam, T.P.A. Anticancer property of gallic acid in A549, a human lung adenocarcinoma cell line, and possible mechanisms. *J. Clin. Biochem. Nutr.* **2011**, *48*, 85–90. [[CrossRef](#)]
21. Faried, A.; Kurnia, D.; Faried, L.S.; Usman, N.; Miyazaki, T.; Kato, H. Anticancer effects of gallic acid isolated from Indonesian herbal medicine, *Phaleria macrocarpa* (Scheff.) Boerl, on human cancer cell lines. *Int. J. Oncol.* **2007**, *30*, 605–613.
22. Zhang, T.; Ma, L.; Wu, P.; Li, W.; Li, T.; Gu, R.; Dan, X.; Li, Z.; Fan, X.; Xiao, Z. Gallic acid has anticancer activity and enhances the anticancer effects of cisplatin in non-small cell lung cancer A549 cells via the JAK/STAT3 signaling pathway. *Oncol. Rep.* **2019**, *41*, 1779–1788. [[CrossRef](#)] [[PubMed](#)]
23. Khorsandi, K.; Kianmehr, Z.; Hosseinmardi, Z.; Hosseinzadeh, R. Anti-cancer effect of gallic acid in presence of low level laser irradiation: ROS production and induction of apoptosis and ferroptosis. *Cancer Cell Int.* **2020**, *20*, 18. [[CrossRef](#)] [[PubMed](#)]
24. Birosova, L.; Mikulasova, M.; Vaverkova, S. Antimutagenic effect of phenolic acids. *Biomed. Pap. Med. Fac. Univ. Palacky. Olomouc Czech Repub.* **2005**, *149*, 489–491. [[CrossRef](#)]
25. Shekaari, H.; Zafarani-Moattar, M.T.; Mokhtarpour, M.; Faraji, S. Solubility of hesperidin drug in aqueous biodegradable acidic choline chloride-based deep eutectic solvents. *Sci. Rep.* **2023**, *13*, 11276. [[CrossRef](#)] [[PubMed](#)]
26. Tung, H.H.; Tabora, J.; Variankaval, N.; Bakken, D.; Chen, C.C. Prediction of pharmaceutical solubility Via NRTL-SAC and COSMO-SAC. *J. Pharm. Sci.* **2008**, *97*, 1813–1820. [[CrossRef](#)]
27. Chen, C.C.; Song, Y. Generalized electrolyte-NRTL model for mixed-solvent electrolyte systems. *Aiche J.* **2004**, *50*, 1928–1941. [[CrossRef](#)]
28. Lin, S.-T.; Sandler, S.I. A Priori Phase Equilibrium Prediction from a Segment Contribution Solvation Model. *Ind. Eng. Chem. Res.* **2002**, *41*, 899–913. [[CrossRef](#)]
29. Chen, Y.; Zhou, S.; Wang, Y.; Li, L. Screening solvents to extract phenol from aqueous solutions by the COSMO-SAC model and extraction process simulation. *Fluid. Phase Equilibria* **2017**, *451*, 12–24. [[CrossRef](#)]
30. Oliveira, G.; Wojeicchowski, J.P.; Farias, F.O.; Igarashi-Mafra, L.; de Pelegrini Soares, R.; Mafra, M.R. Enhancement of biomolecules solubility in aqueous media using designer solvents as additives: An experimental and COSMO-based models' approach. *J. Mol. Liq.* **2020**, *318*, 114266. [[CrossRef](#)]
31. Klamt, A. Conductor-like Screening Model for Real Solvents: A New Approach to the Quantitative Calculation of Solvation Phenomena. *J. Phys. Chem.* **1995**, *99*, 2224–2235. [[CrossRef](#)]
32. Shah, M.R.; Yadav, G.D. Prediction of liquid–liquid equilibria of (aromatic + aliphatic + ionic liquid) systems using the Cosmo-SAC model. *J. Chem. Thermodyn.* **2012**, *49*, 62–69. [[CrossRef](#)]
33. Silveira, C.L.; Galvão, A.C.; Robazza, W.S.; Feyh, J.V.T. Modeling and parameters estimation for the solubility calculations of nicotinamide using UNIFAC and COSMO-based models. *Fluid. Phase Equilibria* **2021**, *535*, 112970. [[CrossRef](#)]
34. van Krevelen, D.W.; Nijenhues, K.T. *Properties of Polymers*, 4th ed.; Elsevier: Amsterdam, The Netherlands, 2009.
35. Wang, S.; Sandler, S.I.; Chen, C.-C. Refinement of COSMO-SAC and the Applications. *Industrial Eng. Chem. Res.* **2007**, *46*, 7275–7288. [[CrossRef](#)]
36. Morcelli, A.; Cassel, E.; Vargas, R.; Rech, R.; Marcilio, N. Supercritical fluid (CO₂+ethanol) extraction of chlorophylls and carotenoids from *Chlorella sorokiniana*: COSMO-SAC assisted prediction of properties and experimental approach. *J. CO₂ Util.* **2021**, *51*, 101649. [[CrossRef](#)]
37. Lee, B.-S.; Lin, S.-T. Prediction and Screening of Solubility of Pharmaceuticals in Single- and Mixed-Ionic Liquids Using COSMO-SAC Model. *Aiche J.* **2017**, *63*, 3096–3104. [[CrossRef](#)]
38. Sandler, S.I. *Chemical, Biochemical, and Engineering Thermodynamics*, 4th ed.; John Wiley & Sons, Inc.: Hoboken, NJ, USA, 2006.
39. Hsieh, C.M.; Sandler, S.I.; Lin, S.T. Improvements of COSMO-SAC for vapor-liquid and liquid-liquid equilibrium predictions. *Fluid. Phase Equilib.* **2010**, *297*, 90–97. [[CrossRef](#)]
40. Staverman, A.J. The entropy of high polymer solutions. Generalization of formulae. *Recl. Des. Trav. Chim. Des. Pays-Bas* **1950**, *69*, 163–174. [[CrossRef](#)]
41. Hildebrand, J.H.; Scott, R.L. Solutions of nonelectrolytes. *Annu. Rev. Phys. Chem.* **1950**, *1*, 75–92. [[CrossRef](#)]
42. Hansen, C.M. *Hansen Solubility Parameters: A User's Handbook*; CRC Press LLC: Boca Raton, FL, USA, 2000; pp. 1–26.
43. Radmand, S.; Rezaei, H.; Zhao, H.; Rahimpour, E.; Jouyban, A. Solubility and thermodynamic study of deferiprone in propylene glycol and ethanol mixture. *BMC Chem.* **2023**, *17*, 37. [[CrossRef](#)]
44. Xue, N.; He, B.; Jia, Y.; Yang, C.; Wang, J.; Li, M. The mechanism of binding with the alpha-glucosidase in vitro and the evaluation on hypoglycemic effect in vivo: Cocrystals involving synergism of gallic acid and conformer. *Eur. J. Pharm. Biopharm.* **2020**, *156*, 64–74. [[CrossRef](#)]
45. Sagdicoglu Celep, A.G.; Demirkaya, A.; Solak, E.K. Antioxidant and anticancer activities of gallic acid loaded sodium alginate microspheres on colon cancer. *Curr. Appl. Phys.* **2022**, *40*, 30–42. [[CrossRef](#)]

46. Singh, D.; Singh Maniyari Rawat, M.; Semalty, A.; Semalty, M. Gallic Acid-Phospholipid Complex: Drug Incorporation and Physicochemical Characterization. *Lett. Drug Des. Discov.* **2011**, *8*, 284–291. [[CrossRef](#)]
47. Taylor, B.N.; Kuyatt, C.E. *Guidelines for Evaluating and Expressing the Uncertainty of NIST Measurement Results*; US Department of Commerce: Gaithersburg, MD, USA, 2001. Available online: <https://physics.nist.gov/TN1297> (accessed on 10 January 2024).
48. Joback, K.G.; Reid, R.C. Estimation of Pure-Component Properties from Group-Contributions. *Chem. Eng. Commun.* **2007**, *57*, 233–243. [[CrossRef](#)]
49. Lu, L.-L.; Lu, X.-Y. Solubilities of Gallic Acid and Its Esters in Water. *J. Chem. Eng. Data* **2007**, *52*, 37–39. [[CrossRef](#)]
50. Daneshfar, A.; Ghaziaskar, H.S.; Homayoun, N. Solubility of Gallic Acid in Methanol, Ethanol, Water, and Ethyl Acetate. *J. Chem. Eng. Data* **2008**, *53*, 776–778. [[CrossRef](#)]
51. Mota, F.L.; Queimada, A.J.; Pinho, S.P.; Macedo, E.A. Aqueous Solubility of Some Natural Phenolic Compounds. *Industrial Eng. Chem. Res.* **2008**, *47*, 5182–5189. [[CrossRef](#)]
52. Dali, I.; Aydi, A.; Alberto, C.C.; Wüst, Z.A.; Manef, A. Correlation and semi-empirical modeling of solubility of gallic acid in different pure solvents and in binary solvent mixtures of propan-1-ol + water, propan-2-ol + water and acetonitrile + water from (293.2 to 318.2) K. *J. Mol. Liq.* **2016**, *222*, 503–519. [[CrossRef](#)]
53. Dabir, T.O.; Gaikar, V.G.; Jayaraman, S.; Mukherjee, S. Thermodynamic modeling studies of aqueous solubility of caffeine, gallic acid and their cocrystal in the temperature range of 303 K–363 K. *Fluid. Phase Equilibria* **2018**, *456*, 65–76. [[CrossRef](#)]
54. Vilas-Boas, S.M.; Brandão, P.; Martins, M.A.R.; Silva, L.P.; Schreiner, T.B.; Fernandes, L.; Ferreira, O.; Pinho, S.P. Solubility and solid phase studies of isomeric phenolic acids in pure solvents. *J. Mol. Liq.* **2018**, *272*, 1048–1057. [[CrossRef](#)]
55. Noubigh, A.; Jeribi, C.; Mgaidi, A.; Abderrabba, M. Solubility of gallic acid in liquid mixtures of (ethanol+water) from (293.15 to 318.15)K. *J. Chem. Thermodyn.* **2012**, *55*, 75–78. [[CrossRef](#)]
56. Klamt, A.; Schuurmann, G. COSMO: A new approach to dielectric screening in solvents with explicit expressions for the screening energy and its gradient. *J. Chem. Soc. Perkin Trans.* **1993**, *2*, 799–805. [[CrossRef](#)]
57. Mahmoudabadi, S.Z.; Pazuki, G. Investigation of COSMO-SAC model for solubility and cocrystal formation of pharmaceutical compounds. *Sci. Rep.* **2020**, *10*, 19879. [[CrossRef](#)] [[PubMed](#)]
58. Barton, A.F.M. *Handbook of Polymer-Liquid Interaction Parameters and Solubility Parameters*; Routledge: New York, NY, USA, 1990.
59. Tirado, D.F.; Tenorio, M.J.; Cabañas, A.; Calvo, L. Prediction of the best cosolvents to solubilise fatty acids in supercritical CO₂ using the Hansen solubility theory. *Chem. Eng. Sci.* **2018**, *190*, 14–20. [[CrossRef](#)]

Disclaimer/Publisher's Note: The statements, opinions and data contained in all publications are solely those of the individual author(s) and contributor(s) and not of MDPI and/or the editor(s). MDPI and/or the editor(s) disclaim responsibility for any injury to people or property resulting from any ideas, methods, instructions or products referred to in the content.